

## LINEAR SPECTRAL MIXTURE ANALYSIS OF TM DATA FOR LAND-USE AND LAND-COVER CLASSIFICATION IN RONDÔNIA, BRAZILIAN AMAZON

Dengsheng Lu,<sup>1</sup> Mateus Batistella,<sup>2,3</sup> and Emilio Moran<sup>1,2</sup>

<sup>1</sup>Center for the Study of Institutions, Population, and Environmental Change (CIPEC)  
Indiana University, Bloomington, Indiana, USA  
Telephone: 812-856-5767, Fax: 812-855-2634  
E-mail: dlu@indiana.edu

<sup>2</sup>Anthropological Center for Training and Research on Global Environmental Change (ACT)  
Indiana University, Bloomington, Indiana, USA

<sup>3</sup>Brazilian Agricultural Research Corporation, EMBRAPA Satellite Monitoring  
Campinas, São Paulo, Brazil

### Commission IV

**KEY WORDS:** linear spectral mixture analysis, land use, land cover, classification, Thematic Mapper, Brazilian Amazon

### ABSTRACT:

The mixed pixels in remotely sensed data are one of the main error sources resulting in poor classification accuracy using traditional classification methods. In order to improve classification accuracy, linear spectral mixture analysis (LSMA) has been used to handle the mixed pixel problems. This paper aims to achieve an appropriate processing routine of LSMA through the comparison of classification results derived from different processing methods, i.e., constrained and unconstrained least-square solutions, different numbers of endmembers, different image bands used, and minimum noise fraction (MNF) transformation. A Landsat Thematic Mapper (TM) image of June 18, 1998, was used, and field data were collected in Rondônia, Brazilian Amazon. Seven classes are defined: mature forest, intermediate secondary succession (SS2), initial secondary succession (SS1), pasture, agriculture, water, and bare land (including urban areas, roads, and bare soil for cultivation). This study indicates that using constrained or unconstrained least-square solutions, atmospherically corrected or raw TM images in LSMA do not produce significant difference in the overall classification accuracy. However, reducing correction between image bands used in LSMA is useful in improving fraction quality and classification accuracy. Selection of four endmembers (green vegetation, shade, bright soil, and dark soil) and bands TM 3, 4, 5, and 7 provided the best classification accuracy. The overall classification accuracy reached 86%. This study shows that selecting appropriate endmembers and image bands is crucial for developing high quality fraction images using LSMA.

### INTRODUCTION

Mixed pixels are common in remotely sensed data because of limitations in spatial resolution of the data and the heterogeneity of features on the ground. The mixture spectra are often generated when the pixel covers more than one land-cover class. This problem often produces poor classification accuracy when conventional algorithms such as the maximum likelihood classifier (MLC) are used. In moist tropical regions, classification of stages of secondary succession (SS) is especially difficult because of its variations in vegetation stand structure, species composition, and biomass (Mausel et al., 1993). However, it is possible to obtain better results if the mixed pixels are decomposed into different proportions of selected components. In order to solve the mixed pixel problem, scientists have developed different models to unmix the pixels into different proportions of the endmembers (Ichoku and Karnieli, 1996). Linear spectral mixture analysis (LSMA) is one of the most often used methods for handling the spectral mixture problem. It assumes that the spectrum measured by a sensor is a linear combination of the spectra of all components within the pixel (Roberts et al., 1998; Ustin et al., 1998). LSMA is a physically based image analysis process that supports repeatable and accurate extraction of quantitative subpixel information (Adams et al., 1986; Smith et al., 1990; Roberts et al., 1998; Ustin et al., 1999). It has been used for vegetation or land-cover classification (Ustin et al., 1996; Cochrane and

Souza, 1998; Aguiar et al., 1999; Petrou, 1999; Ustin et al., 1999; DeFries et al., 2000; Ustin and Xiao, 2001; Theseira et al., 2002) and for change detection (Adams et al., 1995; Roberts et al., 1997; Roberts et al., 1998; Ustin et al., 1998; Elmore et al., 2000; Rogan et al., 2002).

Although LSMA has been recognized as an effective method in handling spectral mixture problems, some uncertainties are still not fully understood. For example, which unmixing solutions (e.g., constrained and unconstrained least-square solutions) can improve the quality of fraction images? How many endmembers are suitable for land-use and land-cover (LULC) classification? Can image transformation (e.g., minimum noise fraction or MNF) improve the fraction quality? Is atmospheric correction of remotely sensed data required before using LSMA? This paper contributes to these debates through comparisons of LULC classification results based on fraction images, which are developed from different image processing routines in Rondônia, Brazilian Amazon.

### STUDY AREA AND FIELD DATA COLLECTION

Rondônia has had the highest deforestation rate in the Brazilian Amazon during the last twenty years (Dale and Pearson, 1997). Following the national strategy of regional occupation and development, colonization projects initiated by the Brazilian

government in the 1970s played a major role in this process (Schmink and Wood, 1992). Most colonization projects in the state were designed to settle landless migrants. Settlement began in this area in the mid-1980s, and the immigrants transformed the landscape into a mosaic of forest remnants, cultivated crops, pastures, and fallow land. The data used in this study were collected in Machadinho d'Oeste in northeastern Rondônia (Figure 1). The climate in Machadinho d'Oeste is classified as equatorial hot and humid, with tropical transition. The well-defined dry season lasts from June to August, and the annual average precipitation is 2,016.6 mm (Rondônia, 1998). The annual average temperature is 25.5°C, and monthly averages for air moisture range from 80 to 85 percent. The terrain is undulated, ranging from 100 m to 450 m above sea level. Several soil types were identified, mainly alfisols, oxisols, ultisols, alluvial soils, and other less spatially represented associations (Miranda and Mattos, 1993). Settlers, rubber tappers, and loggers inhabit the area, transforming the landscape through their economic activities and use of resources.

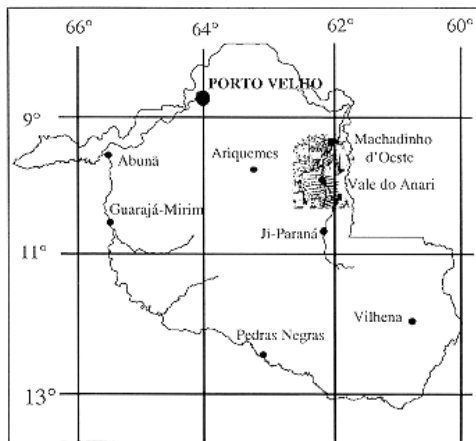


Figure 1. Location of Machadinho d'Oeste in the State of Rondônia, Brazilian Amazon

Field data were collected in the dry season of 1999 and 2000. Preliminary image classification and band composite printouts indicated candidate areas to be surveyed, and a flight over the areas provided visual insights about the size, condition, and accessibility of each site. After driving extensively throughout the settlements, field observations gave a sense about the structure of regrowth stages, mainly regarding total height and ground cover of dominant species. Indicator species, such as *Cecropia sp.*, *Vismia sp.*, palms, grassy vegetation, and lianas also helped to assign the SS stages. Every plot was registered with a Global Positioning System (GPS) device to allow integration with spatial data in Geographic Information Systems (GIS) and image processing systems. Detailed information regarding data gathering can be found in Batistella (2001). The field data were randomly separated into two groups. One group was used for training data for supervised classification, and another group was used for accuracy assessment.

#### LULC CLASSIFICATION USING LSMA

The application of LSMA to LULC classification involves image preprocessing, endmember selection, constrained or unconstrained least-square unmixing solutions, and classification. TM imagery for June 18, 1998, was

radiometrically and atmospherically calibrated into surface reflectance using an improved image-based DOS model (Lu et al., in press). The image was geometrically rectified based on control points taken from topographic sheets at 1:100,000 scale (UTM south 20 zone). Nearest-neighbor resampling technique was used. The root-mean-square (RMS) error was smaller than 0.5 pixel.

A variety of methods were used to determine endmembers (Smith et al., 1990; Quarmby et al., 1992; Boardman, 1993; Roberts et al., 1993; Settle and Drake, 1993; Boardman et al., 1995; Bateson and Curtiss, 1996). Some previous literature has also discussed and summarized the methods of endmember selection (Adams et al., 1993; Tompkins et al., 1997; Mustard and Sunshine, 1999). For many applications of LSMA, image endmembers are often used because they can be obtained easily, representing spectra measured at the same scale as the image data (Roberts et al., 1998). Image endmembers were derived from the extremes of the image feature space, assumed to represent the purest pixels in the images (Roberts et al., 1998; Mustard and Sunshine, 1999). Three endmembers (shade, soil, and green vegetation or GV) were identified from the scattergram of bands TM 3 and TM 4 and scattergram of bands TM 4 and TM 5. An average of 4 to 10 pixels of these vertices was calculated. When selecting the endmembers, cautions need to be taken to identify outliers.

In order to develop high-quality fraction images, different image transformations can be used (Cochrane and Souza, 1998; Van der Meer and de Jong, 2000). The MNF transformation is one of the often used methods for reducing redundancy of information between image bands and assisting selection of endmembers. In this paper, the main objective is to find a proper image processing method for LULC classification using LSMA. Therefore, six different processing methods were tested and their classification results were compared. The following routines were defined:

1. Raw-c: using constrained LSMA method with three endmembers (GV, shade, and soil) on raw six-band TM image;
2. Ref-c: using constrained LSMA method with three endmembers on six-band TM reflectance image;
3. Ref-uc: using unconstrained LSMA method with three endmembers on six-band TM reflectance image;
4. MNF-c: using constrained LSMA method with three endmembers on the first four MNF components;
5. Subset-c: using constrained LSMA method with three endmembers on image band subset (bands TM 3, 4, 5, and 7); and
6. Subset-4c: using constrained LSMA method with four endmembers (GV, shade, bright soil, and dark soil) on image band subset (bands TM 3, 4, 5, and 7).

Seven LULC classes—mature forest (MF), intermediate secondary succession (SS2), initial secondary succession (SS1), pasture (including cultivated and degraded pastures), agriculture (including coffee and cacao plantations and other crops), water, and bare land (including urban areas, roads, and bare soil for cultivation)—were defined according to the LULC characteristics of the study area. The classification was conducted on the fraction images using a maximum likelihood classifier.

Error matrices are often used to assess classification accuracy by comparing the relationships between ground-truth data (reference data) and classified results (Congalton, 1991; Janssen and Van der Wel, 1994; Jensen, 1996; Smits et al., 1999). Producer's accuracy (a measure of omission error) and

user's accuracy (a measure of commission error) were calculated based on error matrices. The reference data covering different LULC classes were collected during fieldwork. These data were linked to the TM image, using the IMAGINE AOI (area of interest) tool to create test samples. Each AOI was associated with an integer number corresponding to a given LULC class. Then, a reference data image was created and compared to the classified image pixel by pixel to create the error matrix table for accuracy assessment.

## RESULTS AND DISCUSSION

The endmember fractions were developed using LSMA based on different image processing routines. Figure 2 gives an example illustrating the fraction characteristics of some typical LULC classes in the study area. In the soil fraction, bare land has significantly higher values, while different successional and mature forests have very small fraction values. Pastures and agriculture such as coffee plantations have relative higher fraction values than those of successional and mature forests. In the GV fraction, water and bare land have small fraction values. Mature forest has the lowest GV fraction values (after bare land and water), and SS1 has the highest GV fraction values. In the shade fraction, water has the highest value and bare land the lowest value. Mature forest has significantly higher fraction value, and SS1 and pastures have lower fraction values. SS2 and agriculture have lower values than mature forest but higher values than pasture and SS1. The error fraction indicates that high quality fraction images are obtained and the results are reliable because the error value for all LULC classes is very small. This figure indicates that water and bare land are the two classes that have the most different characteristics in the fraction image compared with any other LULC classes. The distinction between vegetation types (SS and mature forest) and pasture or agricultural land is better in the soil fraction, but the distinction between different SS stages and mature forest or between pasture and agriculture is better in the GV and shade fractions. Other fraction images derived from different image processing routines have similar trends in distinguishing LULC classes.

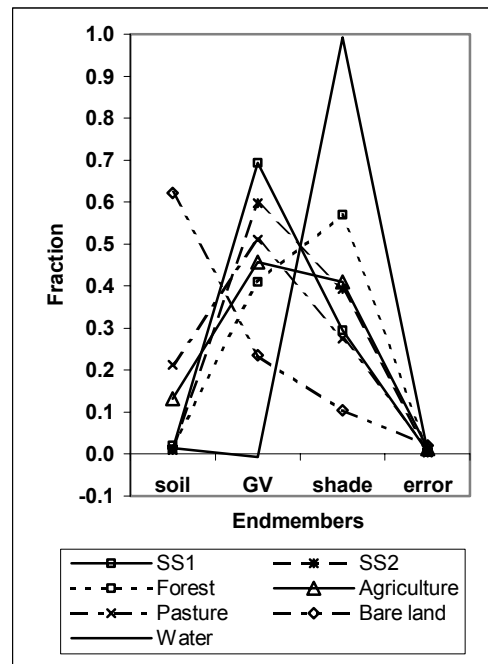


Figure 2. Fraction values of typical LULC classes in Rondônia

Table 1 summarizes the classification accuracies using different processing routines. Concerning atmospheric correction or not, the RAW-c produced 0.9% higher overall accuracy than Ref-c. This implies that atmospheric correction of TM images cannot improve classification or such correction is not required for LSMA application to LULC classification when image endmembers are used. The RAW-c method provides a slightly better accuracy for pasture and bare land, but the Ref-c method provides a little better accuracy for successional classes.

Table 1. Comparison of classification accuracy derived from different processing routines

| LULC Classes | Different Image Processing Routines |       |        |       |        |       |       |       |          |       |           |       |
|--------------|-------------------------------------|-------|--------|-------|--------|-------|-------|-------|----------|-------|-----------|-------|
|              | Raw-c                               |       | Ref-c  |       | Ref-uc |       | MNF-c |       | Subset-c |       | Subset-4c |       |
|              | UA                                  | PA    | UA     | PA    | UA     | PA    | UA    | PA    | UA       | PA    | UA        | PA    |
| Forest       | 96.04                               | 99.65 | 95.82  | 99.53 | 95.71  | 99.53 | 95.67 | 98.59 | 95.98    | 99.41 | 95.73     | 98.77 |
| SS2          | 35.89                               | 52.58 | 35.66  | 57.74 | 35.83  | 57.10 | 37.42 | 52.73 | 36.04    | 61.61 | 35.02     | 62.58 |
| SS1          | 85.08                               | 64.30 | 94.15  | 62.51 | 93.87  | 64.00 | 89.55 | 69.12 | 92.52    | 64.68 | 91.43     | 70.95 |
| Pasture      | 78.41                               | 88.68 | 79.47  | 83.53 | 80.52  | 79.38 | 86.48 | 86.37 | 81.17    | 89.08 | 84.96     | 89.02 |
| Agriculture  | 85.03                               | 76.03 | 77.23  | 80.17 | 77.09  | 82.31 | 68.24 | 78.84 | 82.78    | 77.85 | 87.71     | 84.96 |
| Bare land    | 94.72                               | 93.49 | 73.45  | 96.08 | 65.61  | 97.40 | 86.67 | 94.79 | 86.87    | 95.04 | 98.22     | 86.68 |
| Water        | 100.00                              | 80.91 | 100.00 | 74.55 | 100.00 | 71.82 | 97.75 | 79.09 | 100.00   | 73.64 | 100.00    | 92.73 |
| OA           | 83.26                               |       | 82.34  |       | 81.83  |       | 83.93 |       | 84.11    |       | 85.90     |       |

Note: UA = user's accuracy, PA = producer's accuracy, and OA = overall accuracy in percent.

With a constrained or unconstrained least-square solution, the Ref-c and Ref-uc did not produce significantly different overall classification accuracy, although Ref-c has 0.5% higher accuracy than Ref-uc. The Ref-c provided a little better accuracy for bare land, but the accuracy for other classes between Ref-c and Ref-uc is very similar. Concerning image transformation or not, MNF-c produces 1.6% higher overall classification accuracy than that of Ref-c. This implies that image transformation is helpful in improving the separability of

LULC classes. MNF transformation mainly improves the pasture and bare land classification accuracy. For image bands used in LSMA, Subset-c provides 1.8% better overall accuracy than Ref-c. This implies that removal of highly correlated image bands such as TM 1 and TM 2 in LSMA improved the quality of fraction images. The Subset-c method mainly improves pasture, SS2, and bare land accuracy. Concerning how many endmembers are used, the Subset-4c provides 1.8% better overall classification accuracy than Subset-c. The Subset-

4c method mainly improves SS1, pasture, and agriculture accuracy. This implies that adding one more soil endmember can improve those classes for which soil conditions directly affect their reflectance.

The preceding analysis indicates that (1) selecting appropriate image bands through image transformation or removal of highly correlated bands and (2) identifying a sufficient number of endmembers are critical for improving the fraction quality and classification accuracy. On the other hand, the results also indicate that confusion mainly occurred between SS1 and SS2 and among SS1, pasture (e.g., degraded pasture), and agriculture (e.g., coffee plantation). In this study area, the majority of successional vegetation is less than 10 years old on the 1998 TM image. The subclasses for succession were artificially defined based on ground-truth data and TM reflectance. Most of the SS2 vegetation was between 8 and 10 years old, and most of SS1 was less than 8 years old. This leads to poor classification accuracy of SS2 because of the high confusion between old SS1 vegetation and SS2. In practice, the transition between SS1 and SS2 is very smooth and no distinct boundary exists. Also, SS1 is often confused with degraded pasture and some economic agricultural crops, such as coffee plantations. The confusion between bare land and pasture becomes worse with overgrazing during the dry season, when soil spectral response contributes more significantly to the signature of sparsely covered grassy vegetation. On the other hand, degraded pasture in the process of vegetation recovery often has high densities of *Vismia sp.* and *Orbignya sp.*, increasing the confusion with the spectral response for SS1 or even perennial agriculture. Spectral responses for perennial agriculture can also be confused with SS1, mainly in areas of initial recovery of disturbed gallery vegetation.

In the moist tropical forest, vegetation stand structure and species composition are very complex. For an optical satellite sensor such as Landsat TM, the sensor mainly captures the leaves, wood, and shadowing information for a dense vegetation area. But for sparse vegetation, soil, and litter also affect the reflectance. In a large study area, soil conditions can be different, and the impacts of soil on reflectance can vary. Not all components selected are resolvable in a given image because of the particular mixture and their spectral contrasts. Different study purposes and different characteristics of selected study areas will require different endmembers. The selection of endmembers can be refined based on the analysis of the error fraction or unmodeled spectral variance. For TM images, selecting more than four endmembers is often difficult based on the image itself. Also, high correlation between TM bands limits the number of endmembers that can be used in LSMA.

## CONCLUSIONS

This study indicated that LSMA is a promising approach for LULC classification in the Amazon. The soil fraction helps better distinguish successional and mature forests from pastures and agricultural lands. Green vegetation and shade fractions better distinguish mature forests from successional forests and pastures from agricultural lands. Based on the classification results, the following conclusions were achieved:

1. Constrained or unconstrained least-square unmixing solutions and atmospherically corrected or raw TM images do not produce significantly different overall classification accuracy. The overall accuracy was between 81.8% and 83.3%.

2. MNF transformation improved the overall accuracy, especially for pasture classes and bare land. An overall accuracy of 83.9% was achieved when using this technique, a 1.6% increase compared with the Ref-c method.
3. TM band subset images (bands TM 3, 4, 5, and 7) improved the accuracy for SS2, pasture, and bare land. An overall accuracy of 84.1% was achieved in this case.
4. Four endmembers (GV, shade, bright soil, and dark soil) with TM band subsets (TM 3, 4, 5, and 7) improved the accuracy for SS1, pasture, and agriculture. The overall accuracy reached 85.9% when using this approach.

In summary, selecting endmembers appropriately and reducing correlation between image bands used are two crucial aspects for developing high-quality fraction images when LSMA is used for LULC classification.

## ACKNOWLEDGEMENTS

The authors wish to thank the National Science Foundation (grants 95-21918 and 99-06826), the National Aeronautics and Space Administration (grant N005-334), and Brazil's CAPES (Program for the Advancement of Education) for their support, which provided funds for the research that led to this paper. This project is part of the Large-Scale Biosphere-Atmosphere Experiment in Amazonia (LBA) program, LC-09, examining the human and physical dimensions of land-use and land-cover change. We also thank Indiana State University and Indiana University for facilities and support of our work and collaborators in Brazil, especially the LBA Program, EMBRAPA Satellite Monitoring, and the population of the study area, who made this work possible. We also appreciate the editing done by Joanna Broderick. None of the above funding organizations or individuals should be held responsible for the views presented in this paper. Sole responsibility for content lies with the authors.

## REFERENCES

- Adams, J.B., D.E. Sabol, V. Kapos, R.A. Filho, D.A. Roberts, M.O. Smith, and A.R. Gillespie, 1995. Classification of multispectral images based on fractions of endmembers: application to land cover change in the Brazilian Amazon. *Remote Sensing of Environment*, 52, pp. 137–154.
- Adams, J.B., M.O. Smith, and A.R. Gillespie, 1993. Imaging spectroscopy: interpretation based on spectral mixture analysis. In: *Remote Geochemical Analysis, Topics in Remote Sensing 4*, ed. C.M. Pieters and P.A.J. Englert, Cambridge University Press, Cambridge, U.K., pp.145–166.
- Adams, J.B., M.O. Smith, and P.E. Johnson, 1986. Spectral mixture modeling: a new analysis of rock and soil types at the Viking Landser 1 site. *Journal of Geophysical Research*, 91, pp. 8098–8112.
- Aguiar, A.P.D., Y.E. Shimabukuro, and N.D.A. Mascarenhas, 1999. Use of synthetic bands derived from mixing models in the multispectral classification of remote sensing images. *International Journal of Remote Sensing*, 20, pp. 647–657.
- Bateson, A., and B. Curtiss, 1996. A method for manual endmember selection and spectral unmixing. *Remote Sensing of Environment*, 55, pp. 229–243.

- Batistella, M., 2001. *Landscape change and land-use/land-cover dynamics in Rondônia, Brazilian Amazon*. Ph.D. diss., Indiana University, Bloomington, Ind. USA, 399 pp.
- Boardman, J.M., 1993. Automated spectral unmixing of AVIRIS data using convex geometry concepts. In: *Summaries of the Fourth JPL Airborne Geoscience Workshop*, JPL Publication 93-26, Jet Propulsion Laboratory, Calif., USA, pp.11–14.
- Boardman, J.M., F.A. Kruse, and R.O. Green, 1995. Mapping target signature via partial unmixing of AVIRIS data. In: *Summaries of the Fifth JPL Airborne Earth Science Workshop*, JPL Publication 95-1, Jet Propulsion Laboratory, Calif., USA, pp.23–26.
- Cochrane, M.A., and C.M. Souza Jr., 1998. Linear mixture model classification of burned forests in the eastern Amazon. *International Journal of Remote Sensing*, 19, pp. 3433–3440.
- Congalton, R.G., 1991. A review of assessing the accuracy of classification of remotely sensed data. *Remote Sensing of Environment*, 37, pp. 35–46.
- Dale, V.H., and S.M. Pearson, 1997. Quantifying habitat fragmentation due to land-use change in Amazônia. In: *Tropical Forest Remnants: Ecology, Management, and Conservation of Fragmented Communities*, ed. W.F. Laurance and R.O. Bierregaard Jr., The University of Chicago Press, Chicago, Ill., USA, pp.400–409.
- DeFries, R.S., M.C. Hansen, and J.R.G. Townshend, 2000. Global continuous fields of vegetation characteristics: a linear mixture model applied to multi-year 8km AVHRR data. *International Journal of Remote Sensing*, 21, pp. 1389–1414.
- Elmore, A.J., J.F. Mustard, S.J. Manning, and D.B. Lobell, 2000. Quantifying vegetation change in semiarid environments: precision and accuracy of spectral mixture analysis and the normalized difference vegetation index. *Remote Sensing of Environment*, 73, pp. 87–102.
- Ichoku, C., and A. Karnieli, 1996. A review of mixture modeling techniques for sub-pixel land cover estimation. *Remote Sensing Reviews*, 13, pp. 161–186.
- Janssen, L.F.J., and F.J.M. Van der Wel, 1994. Accuracy assessment of satellite derived land-cover data: a review. *Photogrammetric Engineering and Remote Sensing*, 60, pp. 419–426.
- Jensen, J. R., 1996. *Introduction Digital Image Processing: A Remote Sensing Perspective*, 2d ed. Prentice Hall, New York.
- Lu, D.S., P. Mausel, E.S. Brondizio, and E. Moran, in press. Assessment of atmospheric correction methods for Landsat TM data applicable to Amazon basin LBA research. *International Journal of Remote Sensing*.
- Mausel, P., Y. Wu, Y. Li, E.F. Moran, and E.S. Brondizio, 1993. Spectral identification of succession stages following deforestation in the Amazon. *Geocarto International*, 8, pp. 61–72.
- Miranda, E.E., and C. Mattos, 1993. *Machadinho d'Oeste: de colonos a municípios na floresta tropical de Rondônia*. Ecoforça/Embrapa-NMA, Campinas, Brazil, 154 pp.
- Mustard, J.F., and J.M. Sunshine, 1999. Spectral analysis for earth science: investigations using remote sensing data. In: *Remote Sensing for the Earth Sciences: Manual of Remote Sensing*, 3d ed., v. 3, ed. A.N. Rencz, John Wiley and Sons, New York, pp. 251–307.
- Petrou, M., 1999. Mixed pixel classification: an overview. In: *Information Processing for Remote Sensing*, ed. C.H. Chen, World Scientific Publishing Co., Singapore, pp. 69–83.
- Quarmby, N.A., J.R.G. Townshend, J.J. Settle, and K.H. White, 1992. Linear mixture modeling applied to AVHRR data for crop area estimation. *International Journal of Remote Sensing*, 13, pp. 415–425.
- Roberts, D.A., G.T. Batista, J.L.G. Pereira, E.K. Waller, and B.W. Nelson, 1998. Change identification using multitemporal spectral mixture analysis: applications in eastern Amazonia. In: *Remote Sensing Change Detection: Environmental Monitoring Methods and Applications*, ed. R.S. Lunetta and C.D. Elvidge, Ann Arbor Press, Ann Arbor Mich., USA, pp. 137–161.
- Roberts, D.A., R.O. Green, and J.B. Adams, 1997. Temporal and spatial patterns in vegetation and atmospheric properties from AVIRIS. *Remote Sensing of Environment*, 62, pp. 223–240.
- Roberts, D.A., M.O. Smith, and J.B. Adams, 1993. Green vegetation, non-photosynthetic vegetation, and soils in AVIRIS data. *Remote Sensing of Environment*, 44, pp. 255–269.
- Rogan, J., J. Franklin, and D.A. Roberts, 2002. A comparison of methods for monitoring multitemporal vegetation change using Thematic Mapper imagery. *Remote Sensing of Environment*, 80, pp. 143–156.
- Rondônia, 1998. *Diagnóstico sócio-econômico do Estado de Rondônia e assistência técnica para formulação da segunda aproximação do zoneamento sócio-econômico-ecológico – Climatologia*, v. 1. Governo de Rondônia/PLANAFORO, Porto Velho, Brazil, 401 pp.
- Schmink, M., and C.H. Wood, 1992. *Contested Frontiers in Amazônia*, Columbia University Press, New York, USA.
- Settle, J.J., and N.A. Drake, 1993. Linear mixing and the estimation of ground cover proportions. *International Journal of Remote Sensing*, 14, pp. 1159–1177.
- Smith, M.O., S.L. Ustin, J.B. Adams, and A.R. Gillespie, 1990. Vegetation in deserts: I. A regional measure of abundance from multispectral images. *Remote Sensing of Environment*, 31, pp. 1–26.
- Smits, P.C., S.G. Dellepiane, and R.A. Schowengerdt, 1999. Quality assessment of image classification algorithms for land-cover mapping: a review and a proposal for a cost-based approach. *International Journal of Remote Sensing*, 20, pp. 1461–1486.
- Theseira, M.A., G. Thomas, and C.A.D. Sannier, 2002. An evaluation of spectral mixture modeling applied to a semi-arid environment. *International Journal of Remote Sensing*, 23, pp. 687–700.
- Tompkins, S., J.F. Mustard, C.M. Pieters, and D.W. Forsyth, 1997. Optimization of endmembers for spectral mixture analysis. *Remote Sensing of Environment*, 59, pp. 472–489.

Ustin, S.L., Q.J. Hart, L. Duan, and G. Scheer, 1996. Vegetation mapping on hardwood rangelands in California. *International Journal of Remote Sensing*, 17, pp. 3015–3036.

Ustin, S.L., D.A. Roberts, and Q.J. Hart, 1998. Seasonal vegetation patterns in a California coastal savanna derived from Advanced Visible/Infrared Imaging Spectrometer (AVIRIS) data. In: *Remote Sensing Change Detection: Environmental Monitoring Methods and Applications*, ed. R.S. Lunetta and C.D. Elvidge, Ann Arbor Press, Ann Arbor, Mich., USA, pp. 163–180.

Ustin, S.L., M.O. Smith, S. Jacquemoud, M. Verstraete, and Y. Govaerts, 1999. Geobotany: vegetation mapping for Earth sciences. In: *Remote Sensing for the Earth Sciences: Manual of Remote Sensing*, 3d ed., v. 3, ed. A.N. Rencz, John Wiley and Sons, New York, USA, pp. 189–233.

Ustin, S.L., and Q.F. Xiao, 2001. Mapping successional boreal forests in interior central Alaska. *International Journal of Remote Sensing*, 22, pp. 1779–1797.

Van der Meer, F., and S.M. de Jong, 2000. Improving the results of spectral unmixing of Landsat Thematic Mapper imagery by enhancing the orthogonality of end-members. *International Journal of Remote Sensing*, 21, pp. 2781–2797.